



Kashf Journal of Multidisciplinary Research

Vol: 02 - Issue 09 (2025)

P-ISSN: 3007-1992 E-ISSN: 3007-200X

https://kjmr.com.pk

OPTIMIZING LEAD-FREE CsGeI3 PEROVSKITE SOLAR CELLS: SCAPS-1D SIMULATION ACHIEVING 27.34% EFFICIENCY THROUGH LAYER THICKNESS AND BAND ALIGNMENT TUNING

*Muhammad Yasir Nawaz Khan

Faculty of Sciences, Department of Physics, The Superior University Lahore, Pakistan

Azhar Nawaz

Faculty of Sciences, Department of Physics, The Superior University Lahore, Pakistan

Ayaz Husnain

Faculty of Sciences, Department of Physics, University of Agriculture Faisalabad, Pakistan

Article Info





This article is an open access article distributed under the terms and conditions of the Creative Commons Attribution (CC BY) license

https://creativecommon s.org/licenses/by/4.0

Abstract

Lead-free perovskite solar cells (PSCs) present a sustainable alternative to conventional lead-based devices by mitigating toxicity concerns. In this work, we use SCAPS-1D numerical simulations to optimize an all-inorganic CsGeI3-based PSC structure incorporating TiO2 as the ETL and CuSCN as the HTL. The study systematically explores the influence of absorber thickness (300-700 nm), ETL thickness (50-250 nm), HTL thickness (100-500 nm), and the electron affinities of each layer (CsGeI₃; 3.9-4.1 eV; TiO₂: 4.18-4.34 eV; CuSCN: 1.6-1.8 eV) on device performance. Key photovoltaic parameters V_{OC}, J_{SC}, FF, and PCE are analyzed under these variations. The optimized device achieves a PCE of 27.34%, with $V_{OC} \approx 1.33 \text{ V}$, $J_{SC} \approx 23.59$ mAcm⁻², and FF \approx 86.89%. These enhancements are attributed to efficient charge carrier generation, reduced recombination, and favorable band alignment. The external quantum efficiency approaches 100% across the 390-700 nm wavelength range, indicating strong visible-light absorption. Overall, the results demonstrate the high potential of CsGeI3 for environmentally friendly, high-performance PSCs and provide valuable design guidelines to support experimental realization in renewable energy applications.

Keywords:

Perovskite Solar cell, CsGeI₃, Numerical Simulation, SCAPS 1-D, Inorganic Perovskite, Lead-free Perovskites, TiO₂ ETL, CuSCN HTL

1. INTRODUCTION

Over the past decade, one of the most impactful and revolutionary advancements in the photovoltaic industry has been the rise of perovskite solar cells, which have established themselves as strong competitors to traditional silicon-based solar cells in meeting global energy needs[1]. Compared to other solar cells, PSCs are gaining increasing attention due to their superior optoelectronic properties, excellent absorption coefficient, and easily tunable bandgap, along with their low cost and fabrication through relatively simple processes[2]. Despite their excellent PCE, the presence of toxic lead in PSCs not only raises significant environmental concerns but also poses serious adverse effects on human health[3]. For these reasons, researchers have sought alternatives to toxic lead, and tin has emerged as a promising candidate, being not only non-toxic but also possessing electronic properties comparable to those of lead[4]. However, the easy oxidation of Sn²⁺ to Sn⁴⁺ and the low formation energy of Sn vacancies cause self-doping, which then reduces the overall performance of the cell[5]. Due to all these factors, there was a need for a non-toxic and stable material, which was fulfilled in the form of CsGeI₃, as it is not only stable under ambient conditions but also exhibits superior performance[6]. At ambient temperature, CsGeI₃ was prepared with a rhombohedral structure, achieving a PCE of 0.11%[7]. The bandgap of CsGeI₃ is 1.6 eV, and due to the involvement of Cs or I in its conduction band, it exhibits enhanced performance[8]. Moreover, CsGeI₃ is also utilized as a hole transport material owing to its low hole effective mass and superior band alignment with CH₃NH₃PbI₃[9]. An increase in the thickness of the absorber layer not only boosts the number of charge carriers but also reduces recombination, significantly impacting the cell's performance[10]. Research has shown that using ZnO and CuI as ETL and HTL, respectively, with CsGeI₃ results in a high-performance solar cell, achieving an efficiency of 23.10%[11]. Replacing traditional HTL and ETL materials with n-type and p-type doped CsGel₃ significantly reduces defects, thereby improving cell performance[12]. Studies also show that interfacial defects in the absorber layer impact the overall efficiency of the cell. Additionally, choosing a metal contact with a bandgap between 5 eV and 5.7 eV further enhances device performance, reaching a PCE of up to 22.85%. Researchers boosted the efficiency of a TiO₂/CsGeI₃/MoO₃ solar cell from 19.81% to 22.85% by optimizing key parameters. The cell reached its highest PCE at room temperature, using layer thicknesses of 800 nm for the absorber, 50 nm for MoO₃, and 40 nm for TiO₂. This finding highlights the cell potential for real-world applications[13]. An HTL-free FTO/ZnO/CsGeI₃/W solar cell reached 26.70% PCE and 56.75% FF using tungsten as back contact, reducing recombination with a 0.3 eV barrier. However, JSC was affected by series resistance, and higher defect density increased recombination, harming performance efficiency[14]. ETL and HTL materials are essential in determining cell performance[15], with ETL thickness having a more significant influence than HTL[16]. Studies show that using double ETL layers not only improves cell stability but also decreases charge recombination, leading to a notable increase in PCE. In this work, titanium oxide was chosen because of its excellent band alignment and chemical stability. Its high optical transparency allows for effective light penetration to the absorber layer, resulting in more charge carriers being generated[17]. Spiro-OMeTAD is widely used as an HTL due to its superior performance; however, its low stability and high cost hinder its commercial application [18]. MoO_x, on the other hand, has attracted researchers attention for its greater stability, though ion migration reduces the overall performance of the cell[19]. In this work, CuSCN was selected as the HTL due to its

superior valence band alignment with CsGeI₃, which facilitates efficient hole transport while effectively blocking electrons[20].

2. SIMULATION METHODOLOGY

Numerical simulation, due to its cost-effectiveness and time efficiency, serves as a superior alternative to experimental work. It helps optimize device layers while minimizing fabrication costs and material waste. In this study, the performance of high-efficiency CsGeI₃ perovskite was analyzed using SCAPS-1D simulation software. SCAPS-1D models the behavior of different cell layers by solving the Poisson equation, the continuity equations for holes and electrons, and the current density equation[20]. Our device configuration model includes layers such as transparent conducting oxide (TCO), TiO₂, CsGeI₃, CuSCN, and a back contact. Defined all these layers with their physical and electronic properties, including bandgap energy, electron affinity, dielectric constant, doping concentrations, carrier mobilities, and defect densities, as shown in Table 1. The simulation also used realistic solar illumination (AM 1.5G spectrum)[21], and examine extracted various performance metrics like J-V characteristics, quantum efficiency (QE), open-circuit voltage (Voc), short-circuit current density (JsC), fill factor (FF), and power conversion efficiency (PCE).

Cell Perimeter	CsGeI ₃	CuSCN	TiO ₂
Thicknesses (nm)	300-700	100	30-80
Band gap (eV)	1.6	3.6	3.2
Electron affinity (eV)	3.9	1.7	4.26
Dielectric permittivity	6.5	10	9
CB effective density of state (cm ⁻³)	1.00E18	2.20E19	2.00E18
VB effective density of state (cm ⁻³)	1.00E18	1.80E19	2.20E18
Electron thermal velocity (cms ⁻¹)	1.00E7	1.00E7	1.00E7
Hole thermal velocity (cms ⁻¹)	1.00E7	1.00E7	1.00E7
Electron mobility (cm ² V ⁻¹ s ⁻¹)	50	100	20
Hole mobility (cm ² V ⁻¹ s ⁻¹)	50	25	10
Shallow donor uniform density N _D (cm ⁻³)	0	0	1.00E16
Shallow uniform acceptor density N _A (cm ⁻³)	1.00E16	1.00E18	0
Defect density (N _t)	1.00E15	1.00E14	1.00E15

Table 1. Simulation Perimeter of Each Layer

3. RESULT AND DISCUSSION

3.1 Effect of Thickness of CsGeI₃

The light-harvesting layer plays a significant role in enhancing the performance of the cell, and achieving an optimal thickness of the absorber layer is crucial for improved efficiency[22]. If the absorber layer effectively absorbs photons in the visible wavelength range, the increased generation of charge carriers will lead to higher cell efficiency[23]. In this simulation, the absorber layer thickness was varied from 300 nm to 700 nm, and its effects on the cell's output parameters were analyzed as shown in Table 3. The

results indicated that an increase in thickness led to a rise in the dark saturation current, which caused a slight decrease in $V_{\rm OC}[24]$. However, the photocurrent increased with greater thickness, resulting in an enhancement of $J_{\rm SC}$. A minor improvement in the FF was also observed. At higher thicknesses, the larger number of charge carriers contributed to an increase in PCE, which improved from 22.5184% to 27.2551% shown in Figure 1.

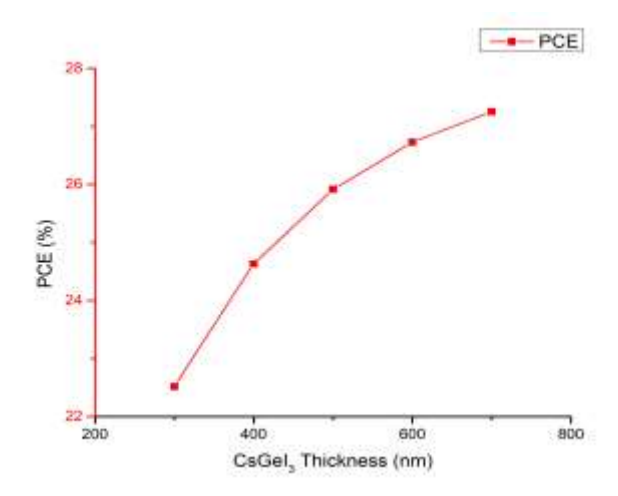


Figure 1. CsGeI₃ Thickness Effect on PCE of Cell

Thickness (nm)	Voc (V)	Jsc (mAcm ⁻²)	FF (%)	PCE (%)
300	1.3627	19.2242	85.9151	22.5184
400	1.353	21.1131	86.224	24.6316
500	1.3453	22.2945	86.4088	25.9171
600	1.339	23.067	86.5372	26.7279
700	1.3337	23.5916	86.6226	27.2551

Table 2. CsGeI₃ Thickness effect on cell output

3.2 Effect of Thickness of TiO₂

To enable the effective transport of electrons and minimize recombination losses, thereby ensuring that the cell performance is not adversely affected, the ETL plays a crucial role. An appropriately optimized ETL thickness enhances charge carrier mobility, which in turn improves the overall performance of the cell[25]. In this simulation, the ETL thickness was varied from 50 nm to 250 nm, and its impact on the device performance was investigated as shown in Table 3. The results revealed that variation in ETL thickness had little effect on the value of V_{OC}, which remained nearly constant. However, due to increased recombination with higher ETL thickness, a slight decrease in J_{SC} was observed. Since recombination increased with greater ETL thickness and the number of effective charge carriers was consequently reduced, both the FF and PCE declined. The optimal thickness at which the maximum PCE was achieved was found to be 50 nm shown in Figure 2.

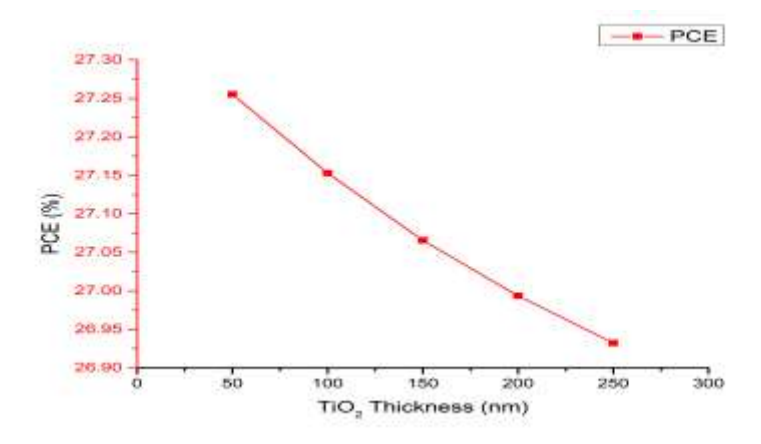


Figure 2. TiO₂ Thickness Effect on PCE of Cell

Thickness nm	Voc (V)	Jsc (mAcm ⁻²)	FF (%)	PCE (%)
50	1.3337	23.5916	86.6226	27.2552
100	1.3335	23.5873	86.3237	27.1531
150	1.3334	23.5774	86.0905	27.0655
200	1.3333	23.556	85.9465	26.9935
250	1.3332	23.5172	85.9005	26.9323

Table 3. TiO₂ Thickness effect on cell output

3.3 Effect of Thickness of CuSCN

For achieving good cell performance, it is essential that holes can easily reach the metal contact while minimizing recombination losses along the path. An efficient hole transport layer (HTL) should possess a suitable bandgap well-aligned with the absorber layer, along with high carrier mobility, to ensure the rapid and efficient transport of charge carriers[26, 27]. In this simulation, the HTL thickness was varied from 100 nm to 500 nm. The results indicated that changes in HTL thickness had no significant impact on the cell's output parameters. All parameters, including the power conversion efficiency (PCE), remained nearly unchanged shown in Table 4.

Thickness nm	Voc (V)	Jsc (mAcm ⁻²)	FF (%)	PCE (%)
100	1.3337	23.5916	86.6226	27.2552
200	1.3337	23.5916	86.6226	27.2553
300	1.3337	23.5916	86.6221	27.2551
400	1.3337	23.5916	86.6225	27.2553
500	1.3337	23.5916	86.6224	27.2552

Table 4. CuSCN Thickness effect on cell output

3.4 Effect of Electron Affinity of CsGeI₃

Electron affinity determines the energy of the conduction band minimum (CBM) relative to a vacuum. Altering EA in a layer shifts its CBM, which in turn changes the conduction-band offset (CBO) at the

absorber/ETL interface [28]. We varied the absorber layer's electron affinity (EA) from 3.9 eV to 4.1 eV and observed its impact on the cell parameters shown in Table 5. The V_{OC} remained approximately constant, which can be attributed to the CBO staying within the near-optimal range. This maintained a balance between photogeneration and dark saturation current, thereby keeping both V_{OC} and J_{SC} stable. As the EA of the absorber increased, the CBO shifted toward a more favorable band alignment, and the maximum PCE was achieved at 4.0 eV. Beyond this point, recombination losses led to a gradual decline in efficiency shown in Figure 3. A similar trend was also observed in the FF.

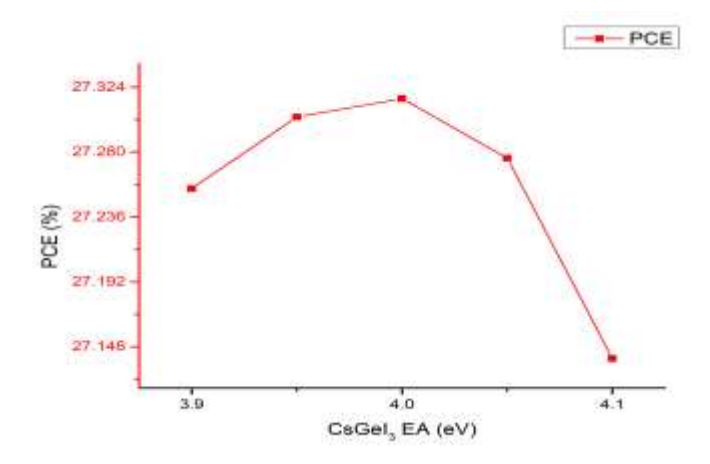


Figure 3.CsGeI₃ EA Effect on PCE of Cell

EA (eV)	Voc (V)	Jsc (mAcm ⁻²)	FF (%)	PCE (%)
3.9	1.3337	23.5916	86.6224	27.2552
3.95	1.3338	23.5891	86.7791	27.3037
4	1.3338	23.5893	86.8179	27.3162
4.05	1.3337	23.5889	86.696	27.2759
4.1	1.3336	23.5892	86.29	27.14

Table 5. CsGeI3 EA effect on cell output

3.5 Effect of Electron Affinity of TiO₂

The conduction band offset (CBO) is determined by the difference in EA between the active layer and the ETL. An optimized CBO facilitates efficient charge extraction, thereby enhancing the PCE of the cell[29]. When the EA of TiO₂ was increased, the conduction band minimum (CBM) of the ETL shifted downward, which reduced the spike at the band alignment interface. As a result, electron extraction improved, leading to an increase in the number of charge carriers and a slight enhancement in the cell's output parameters shown in Table 6[30]. However, with further increases in EA, the PCE became nearly constant shown in Figure 4.

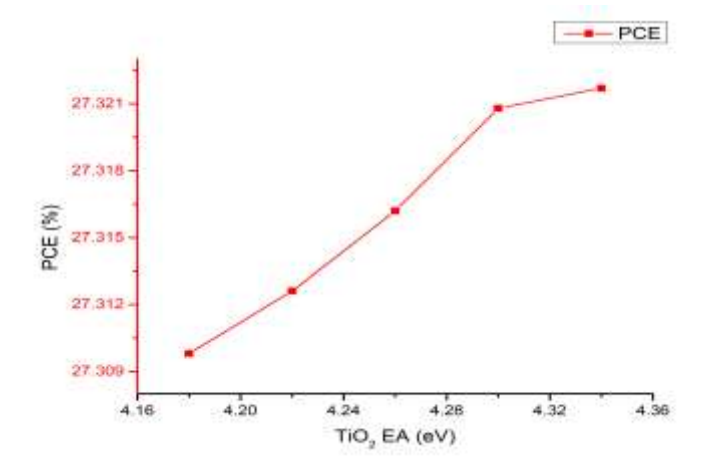


Figure 4. TiO₂ EA Effect on PCE of Cell

EA (eV)	Voc (V)	Jsc (mAcm ⁻²)	FF (%)	PCE (%)
4.18	1.3336	23.5892	86.8112	27.3098
4.22	1.3337	23.5892	86.8126	27.3126
4.26	1.3338	23.5892	86.8179	27.3162
4.3	1.3339	23.5894	86.8269	27.3208
4.34	1.334	23.59	86.8234	27.3217

Table 6. TiO₂ EA effect on cell output

3.6 Effect of electron affinity of CuSCN

Another critical parameter that significantly influences cell performance is the band offset arising from the difference between the bandgaps of the HTL and the absorber layer, referred to as the valence band offset (VBO). Proper adjustment of this offset can reduce recombination, thereby improving the efficiency of the cell[31]. Increasing the EA of the HTL has little effect on the values of V_{OC} and J_{SC} , which remain nearly constant shown in Table 7; however, due to improved band alignment, slight enhancements in both the fill factor FF and the PCE are observed. Beyond an EA value of 1.75 eV, the PCE becomes constant shown in Figure 5.

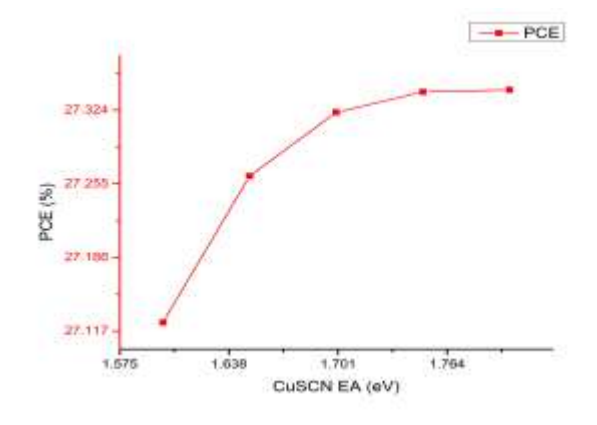


Figure 5.CuSCN EA Effect on PCE of Cell

EA (eV)	Voc (V)	Jsc (mAcm ⁻²)	FF (%)	PCE (%)
1.6	1.334	23.5896	86.1968	27.1251
1.65	1.3346	23.5899	86.6223	27.2622
1.7	1.334	23.59	86.8235	27.3218
1.75	1.3339	23.5904	86.8877	27.341
1.8	1.3338	23.5937	86.8906	27.3429

Table 7.CuSCN EA effect on cell output

3.7 Quantum efficiency of Cell

The rate at which a cell converts incident photons into electric current is referred to as its quantum efficiency. In this study, the cell was simulated over a wavelength range of 300 nm to 900 nm. The results showed that as the wavelength increased beyond 300 nm, the efficiency of the cell also increased, reaching 100% at 390 nm. The cell maintained this performance up to around 700 nm, after which a sudden decline in efficiency was observed, ultimately dropping to zero beyond 800 nm shown in Figure 6. The strong performance of the cell within the visible range highlights its promising potential for practical applications and future technological advancements.

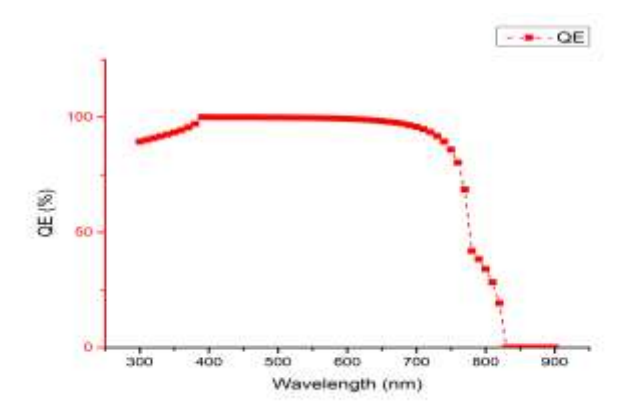


Figure 6. QE of Cell

4. CONCLUSION

This study highlights the strong potential of lead-free, all-inorganic CsGeI₃ perovskite solar cells through systematic SCAPS-1D optimization. Device performance was found to depend critically on absorber thickness, transport layer dimensions, and band alignment. A 700 nm CsGeI₃ absorber ensured efficient light harvesting, while a thin 50 nm TiO₂ ETL minimized recombination. Optimized electron affinities (CsGeI₃: 4.0 eV; CuSCN: 1.75 eV) yielded near-ideal band offsets, enabling effective charge extraction and suppression of losses. The resulting device achieved a peak efficiency of 27.34%, with excellent J_{SC}, V_{OC}, and FF, supported by a broad quantum efficiency spectrum. These results establish CsGeI₃ as a promising candidate for non-toxic, high-performance PSCs and provide a framework for future experimental efforts toward stable, practical devices.

REFERENCES

1. Noman, M., Z. Khan, and S.T. Jan, A comprehensive review on the advancements and challenges in perovskite solar cell technology. RSC advances, 2024. 14(8): p. 5085-5131.

- **2.** Zhang, Y., et al., SCAPS simulation and DFT study of lead-free perovskite solar cells based on CsGeI3. Materials Chemistry and Physics, 2023. 306: p. 128084.
- **3.** Karmaker, H., A. Siddique, and B.K. Das, Numerical investigation of lead free Cs2TiBr6 based perovskite solar cell with optimal selection of electron and hole transport layer through SCAPS-1D simulation. Results in Optics, 2023. 13: p. 100571.
- **4.** Ke, W. and M.G. Kanatzidis, Prospects for low-toxicity lead-free perovskite solar cells. Nature communications, 2019. 10(1): p. 965.
- **5.** Wei, H., et al., Challenges and strategies of all-inorganic lead-free halide perovskite solar cells. Ceramics International, 2022. 48(5): p. 5876-5891.
- **6.** Saikia, D., et al., Performance evaluation of an all inorganic CsGeI3 based perovskite solar cell by numerical simulation. Optical Materials, 2022. 123: p. 111839.
- 7. Krishnamoorthy, T., et al., Lead-free germanium iodide perovskite materials for photovoltaic applications. Journal of Materials Chemistry A, 2015. 3(47): p. 23829-23832.
- **8.** Ravidas, B.K., et al., Design principles of crystalline silicon/CsGeI3 perovskite tandem solar cells using a combination of density functional theory and SCAPS-1D frameworks. Solar Energy Materials and Solar Cells, 2024. 267: p. 112688.
- **9.** Ming, W., H. Shi, and M.-H. Du, Large dielectric constant, high acceptor density, and deep electron traps in perovskite solar cell material CsGeI3. Journal of Materials Chemistry A, 2016. 4(36): p. 13852-13858.
- **10.** Solanki, S., K.V. Bharathi, and K. Bhargava, Fundamental analysis of lead-free CsGeI3 perovskite solar cell. Materials Today: Proceedings, 2022. 67: p. 180-186.
- **11.** Tara, A., et al., Computational approach to explore suitable charge transport layers for all inorganic CsGeI3 perovskite solar cells. Optical Materials, 2022. 128: p. 112403.
- **12.** Lu, J., et al., Replacing the electron-hole transport layer with doping: SCAPS simulation of lead-free germanium-based perovskite solar cells based on CsGeI3. Solar Energy Materials and Solar Cells, 2024. 271: p. 112883.
- **13.** Miah, M.H., et al., Optimization and detail analysis of novel structure Pb-free CsGeI3-based all-inorganic perovskite solar cells by SCAPS-1D. Optik, 2023. 281: p. 170819.
- **14.** Zhang, X., et al., Investigation of efficient all-inorganic HTL-free CsGeI3 perovskite solar cells by device simulation. Materials Today Communications, 2023. 34: p. 105347.

15. Tulka, T.K., et al., Optimization of a high-performance lead-free cesium-based inorganic perovskite solar cell through numerical approach. Heliyon, 2022. 8(11).

- **16.** Song, J., et al., Numerical simulation and performance optimization of all-inorganic CsGeI3 perovskite solar cells with stacked ETLs/C60 by SCAPS device simulation. Materials Today Communications, 2024. 38: p. 108587.
- 17. Raj, A., et al., Effect of doping engineering in TiO2 electron transport layer on photovoltaic performance of perovskite solar cells. Materials Letters, 2022. 313: p. 131692.
- **18.** Sharma, D., R. Mehra, and B. Raj, Optimization of tin based perovskite solar cell employing CuSbS2 as HTL: a numerical simulation approach. Optical Materials, 2022. 134: p. 113060.
- **19.** Anrango-Camacho, C., et al., Recent advances in hole-transporting layers for organic solar cells. Nanomaterials, 2022. 12(3): p. 443.
- **20.** Ahmad, W., et al., Performance analysis and optimization of inverted inorganic CsGeI3 perovskite cells with carbon/copper charge transport materials using SCAPS-1D. Royal Society Open Science, 2023. 10(3): p. 221127.
- **21.** Sabbah, H., Numerical simulation of 30% efficient lead-free perovskite CsSnGeI3-based solar cells. Materials, 2022. 15(9): p. 3229.
- **22.** Singh, N., A. Agarwal, and M. Agarwal, Numerical simulation of highly efficient lead-free all-perovskite tandem solar cell. Solar Energy, 2020. 208: p. 399-410.
- **23.** Li, X., et al., Theoretical analysis of all-inorganic solar cells based on numerical simulation of CsGeI3/CsPbI3 with p-p+ built-in electric field. Solar Energy, 2022. 247: p. 315-329.
- **24.** Sawicka-Chudy, P., et al., Simulation of TiO2/CuO solar cells with SCAPS-1D software. Materials Research Express, 2019. 6(8): p. 085918.
- **25.** Raj, A., et al., A computational approach to investigate the suitable ETL for lead-free CsGeI3 based perovskite solar cell. Materials Today: Proceedings, 2021. 47: p. 1564-1569.
- **26.** Roy, P., Y. Raoui, and A. Khare, Design and simulation of efficient tin based perovskite solar cells through optimization of selective layers: Theoretical insights. Optical Materials, 2022. 125: p. 112057.
- **27.** Pindolia, G., S.M. Shinde, and P.K. Jha, Optimization of an inorganic lead free RbGeI3 based perovskite solar cell by SCAPS-1D simulation. Solar Energy, 2022. 236: p. 802-821.
- **28.** Mozaffari, N., et al., Unraveling the role of energy band alignment and mobile ions on interfacial recombination in perovskite solar cells. Solar RRL, 2022. 6(6): p. 2101087.
- **29.** Minemoto, T., et al., Theoretical analysis of band alignment at back junction in Sn–Ge perovskite solar cells with inverted pin structure. Solar Energy Materials and Solar Cells, 2020. 206: p. 110268.

30. Gan, Y., et al., Numerical Analysis on the Effect of the Conduction Band Offset in Dion–Jacobson Perovskite Solar Cells. Energies, 2023. 16(23): p. 7889.

31. El Arfaoui, Y., M. Khenfouch, and N. Habiballah, Optimization of all Pb-free perovskite CsGeI3/FASnI3 tandem solar device with 30.42% efficiency: numerical simulation using SCAPS. Optik, 2024. 300: p. 171638.